

Large-space cluster model calculations for the ${}^3\text{He}({}^3\text{He}, 2p){}^4\text{He}$ and ${}^3\text{H}({}^3\text{H}, 2n){}^4\text{He}$ reactions

Attila Csótó^{a,b,c}, Karlheinz Langanke^b

^a*Theoretical Division, Los Alamos National Laboratory, Los Alamos, NM 87545, USA*

^b*Institute for Physics and Astronomy, Aarhus University, DK-8000 Aarhus, Denmark*

^c*Department of Atomic Physics, Eötvös University, Pázmány Péter sétány 1/A, H-1117
Budapest, Hungary
(February 9, 2008)*

Abstract

The ${}^3\text{He}({}^3\text{He}, 2p){}^4\text{He}$ and ${}^3\text{H}({}^3\text{H}, 2n){}^4\text{He}$ reactions are studied in a microscopic cluster model. We search for resonances in the ${}^3\text{He}+{}^3\text{He}$ and ${}^4\text{He}+p+p$ channels using methods that treat the two- and three-body resonance asymptotics correctly. Our results show that the existence of a low-energy resonance or virtual state, which could influence the ${}^7\text{Be}$ and ${}^8\text{B}$ solar neutrino fluxes, is rather unlikely. Our calculated ${}^3\text{He}({}^3\text{He}, 2p){}^4\text{He}$ and ${}^3\text{H}({}^3\text{H}, 2n){}^4\text{He}$ cross sections are in a good general agreement with the experimental data.

PACS: 21.45.+v; 25.10.+s; 21.60.Gx; 26.65.t; 27.20.+n

Keywords: Few-body systems; Three-body dynamics; Cluster model; Nuclear astrophysics; Solar neutrinos

I. INTRODUCTION

One way to test models of the solar interior is by observing the neutrinos generated by the nuclear reaction network which is the solar energy source [1]. As a striking and exciting fact, all terrestrial solar neutrino experiments observe fewer neutrinos than predicted by standard solar models [2]. The picture which emerges from the various experiments is [3] that the ^8B flux is about half of its predicted value ($\phi_8 = 0.4\phi_8^{SSM}$), while the ^7Be neutrinos appear to be completely missing ($\phi_7 = 0$). Here SSM refers to the standard solar model of Bahcall [2]. The ^7Be nuclei, which are the seeds of both the ^7Be and ^8B neutrinos, are produced in the $^4\text{He}(^3\text{He}, \gamma)^7\text{Be}$ reaction. This reaction competes with the $^3\text{He}(^3\text{He}, 2p)^4\text{He}$ process, which is the final step of the first branch of solar hydrogen burning (ppI chain) [4]. If the cross section of the $^3\text{He}(^3\text{He}, 2p)^4\text{He}$ reaction were larger than believed then the probability of the $^4\text{He}(^3\text{He}, \gamma)^7\text{Be}$ branch would be smaller, and hence the ϕ_8 and ϕ_7 fluxes would be suppressed (without, however, significantly affecting the unexpected ϕ_7/ϕ_8 ratio deduced from the neutrino experiments [5]). To increase the $^3\text{He}(^3\text{He}, 2p)^4\text{He}$ reaction rate, a hypothetical resonance at low energies had been suggested [6] and looked for in various experiments (see [7] for the most recent work).

The importance of the $^3\text{He}(^3\text{He}, 2p)^4\text{He}$ reaction has led to continued experimental efforts to measure the cross section down to solar energies. In the latest experiment [7] the LUNA collaboration measured the cross section down to $E_{cm} = 20.76$ keV, which is well within the region of the most effective solar energies (Gamow window). Although, they do not see any evidence of a possible resonance, the existence of such a state at still lower energies cannot be *a priori* ruled out yet. In the present work we study the $^3\text{He}(^3\text{He}, 2p)^4\text{He}$ and the mirror $^3\text{H}(^3\text{H}, 2n)^4\text{He}$ reactions in a microscopic cluster model. We search for signs of possible resonances and study the energy dependence of the reaction cross sections.

II. MODEL

The $^3\text{He}(^3\text{He}, 2p)^4\text{He}$ and $^3\text{H}(^3\text{H}, 2n)^4\text{He}$ reactions have already been studied previously within microscopic cluster models [8,9]. We use the same model, but with extended and hence more realistic model spaces. Additionally we put special emphasis on the description of the few-body dynamics. Our model starts out with a resonating group model (RGM) wave function for the $\{^4\text{He} + p + p, ^3\text{He} + ^3\text{He}\}$ coupled system.

$$\begin{aligned} \Psi^{J\pi} = & \sum_{S, l_1, l_2, L} \mathcal{A} \left\{ \left[\left[\Phi^\alpha (\Phi^p \Phi^p) \right]_S \chi_{[l_1 l_2] L}(\boldsymbol{\rho}_1, \boldsymbol{\rho}_2) \right]_{JM} \right\} \\ & + \sum_{S, l_1, l_2, L} \mathcal{A} \left\{ \left[\left[\Phi^p (\Phi^\alpha \Phi^p) \right]_S \chi_{[l_1 l_2] L}(\boldsymbol{\rho}_1, \boldsymbol{\rho}_2) \right]_{JM} \right\} + \mathcal{A} \left\{ \left[\Phi^h \Phi^h \chi_{l_3}(\boldsymbol{\rho}) \right]_{JM} \right\}. \end{aligned} \quad (1)$$

Here \mathcal{A} is the intercluster antisymmetrizer, the Φ cluster internal states are translationally invariant harmonic oscillator shell model states ($\alpha = ^4\text{He}$ and $h = ^3\text{He}$), the $\boldsymbol{\rho}$ vectors are the different intercluster Jacobi coordinates, l_1 and l_2 are the angular momenta of the two relative motions, L and S are the total orbital angular momentum and spin, respectively, J is the total angular momentum, $\pi = (-1)^{l_1+l_2} = (-1)^{l_3}$ is the parity, and [...] denotes angular

momentum coupling. The sum over S, l_1, l_2 , and L includes all physically relevant angular momentum configurations. Using (1) as a trial function in the six-nucleon Schrödinger equation, we arrive at an equation for the intercluster relative motion functions χ . For the mirror $\{^4\text{He} + n + n, ^3\text{H} + ^3\text{H}\}$ system we use a wave function similar to (1). The harmonic oscillator size parameters of the internal cluster states are chosen to stabilize the cluster energies. We use the Minnesota (MN) effective interaction [10] in all calculations. It puts the threshold of the $^3\text{He} + ^3\text{He}$ and $^3\text{H} + ^3\text{H}$ thresholds at 17.11 MeV and 15.57 MeV energies, respectively relative to the $^4\text{He} + N + N$ threshold. Like in the previous studies [8,9], these values are significantly larger than the experimental thresholds (12.86 MeV and 11.33 MeV, respectively). One might expect that the incorrect reproduction of the threshold energies will effect the relative weight of the $^4\text{He} + N + N$ channels in the full wave function. We will briefly discuss this problem below.

The relative motions are the most important degrees of freedom in the problem, so special care has to be taken in order to ensure that their dynamics are described properly. What makes the description of the $^3\text{He}(^3\text{He}, 2p)^4\text{He}$ and its mirror reactions difficult is the fact that there are three particles in the final state continuum. Currently we cannot treat the full three-body continuum problem properly, thus our model is only an approximate description of the reactions. However, the existence of a low-energy resonance in the $^3\text{He}(^3\text{He}, 2p)^4\text{He}$ reaction is a question which can be studied in a rigorous way. If such a resonance existed, it has to originate from either the $^3\text{He} + ^3\text{He}$ or the $^4\text{He} + p + p$ channels. As we will show below, one can investigate the existence of such a resonance in both channels separately and properly. Although we can treat the scattering continuum only approximately, we will nevertheless calculate the low-energy reaction cross sections of the $^3\text{He}(^3\text{He}, 2p)^4\text{He}$ and its mirror reaction.

III. SEARCHING FOR RESONANCES IN $^4\text{He}+p+p$ AND $^3\text{He}+^3\text{He}$

In order to avoid any ambiguity in the recognition of a resonance in real-energy observables, we search for resonances on the complex energy plane. Resonances are defined as the complex-energy solutions of the Schrödinger equation, which correspond to the singularities of the scattering matrix. Thus, we search for poles of both the $^3\text{He} + ^3\text{He}$ and $^4\text{He} + p + p$ S matrices.

Interestingly, the $^4\text{He} + p + p$ case is easier to deal with, despite its three-body nature. The reason is that a low-energy resonance in the $^3\text{He} + ^3\text{He}$ channel corresponds to a high-lying narrow state in the $^4\text{He} + p + p$ channel, which, if it exists, can be easily identified. In order to be able to describe three-body resonances, we apply the complex scaling method (CSM). This method has already been used previously to search for resonances in ^6He , ^6Li , and ^6Be in an $\alpha + N + N$ model [11]. However, the search had been restricted to low-lying resonances below the $^3\text{He} + ^3\text{He}$ threshold and therefore does not shed light on the problem at hand here. In the present search we concentrate on the high-energy region around the $^3\text{He} + ^3\text{He}$ channel threshold. In the CSM the complex scaling transformation is performed on the original Hamiltonian. This transformation acts in coordinate space on a function $f(\mathbf{r})$ as

$$\hat{U}(\theta)f(\mathbf{r}) = e^{3i\theta/2}f(\mathbf{r}e^{i\theta}), \quad (2)$$

where θ is the parameter of the transformation. For real θ values the $\hat{U}(\theta)$ transformation results in a rotation into the complex coordinate plane. The spectrum of the complex-scaled Hamiltonian

$$\hat{H}_\theta = \hat{U}(\theta)\hat{H}\hat{U}^{-1}(\theta) \quad (3)$$

is connected to the spectrum of the original \hat{H} by the following theorem [12]: (i) the bound eigenstates of \hat{H} are eigenstates of \hat{H}_θ , for any value of θ within $0 \leq \theta \leq \pi/2$; (ii) the continuous spectrum of \hat{H} is rotated by an angle 2θ ; (iii) the complex generalized eigenvalues of \hat{H}_θ , $\varepsilon_{\text{res}} = E_r - i\Gamma/2$ (with $E_r, \Gamma > 0$), belong to its proper spectrum, with square-integrable eigenfunctions, provided $2\theta > |\arg \varepsilon_{\text{res}}|$. These complex eigenvalues coincide with the S -matrix pole positions.

We would like to emphasize that this method treats three-body resonances in a rigorous way. The only approximation we make in the present work is that we solve the complex-scaled Schrödinger equation on a finite basis. Namely, we assume that χ in (1) can be expanded in terms of products of Gaussian functions, like $\rho_1^{l_1} \exp[-(\rho_1/\gamma_i)^2] Y_{l_1 m_1}(\hat{\rho}_1) \cdot \rho_2^{l_2} \exp[-(\rho_2/\gamma_j)^2] Y_{l_2 m_2}(\hat{\rho}_2)$, where l_1 and l_2 are the angular momenta in the two relative motions, respectively, and the widths γ of the Gaussians are the parameters of the expansion. The expansion coefficients are determined from the projection equation $\langle \delta\Psi_\theta | \hat{H}_\theta - \varepsilon | \Psi_\theta \rangle = 0$. As the complex-scaled wave function of a resonance is square-integrable, our finite basis approximation works for resonances as well as for bound states.

As an illustrative example of our results, Fig. 1 shows the spectrum of the complex-scaled Hamiltonian for the $J^\pi = 0^+$ state of ${}^4\text{He} + p + p$. We choose a small rotation angle θ in order to avoid any numerical instability. One can see that the well-known ground state resonance of ${}^6\text{Be}$ is reproduced. A low-energy resonance in the ${}^3\text{He}({}^3\text{He}, 2p){}^4\text{He}$ system with small width (which would be relevant for the astrophysical problem), if existed, would be situated above $\text{Re}(E) \approx 10$ MeV, close to the real energy axis. There is no such narrow state present in our model. We do not find such a state in other J^π partial waves either. Our results agree with other calculations performed in a three-body ${}^4\text{He} + N + N$ model assuming structureless ${}^4\text{He}$ [13]. As Ref. [13,14] shows, all high-lying resonances in the ${}^4\text{He} + N + N$ systems have large widths.

In the ${}^3\text{He} + {}^3\text{He}$ channel we cannot use the complex scaling method. A very low-energy resonance would always be mixed up with the rotated continuum, making its unambiguous identification hopeless. Here we use a direct analytic continuation of the S matrix to complex energies [15]. We can use this method because, unlike in the case of the three-body ${}^4\text{He} + p + p$ system, the two-body scattering wave functions can easily be generated with the correct asymptotics. To calculate these scattering wave functions we use the Kohn-Hulthén variational method of Ref. [16]. Once again, our method treats resonances in a rigorous way.

We have searched for low-energy narrow resonances in ${}^3\text{He} + {}^3\text{He}$ and found none. We must note, however, that our ${}^3\text{He} + {}^3\text{He}$ model may be too simple. In the $J^\pi = 0^+$ state, which is the most likely candidate to have a narrow resonance, the singlet S -wave $N - N$ interaction has a dominant effect because the Pauli principle forces the unpaired neutrons inside the ${}^3\text{He}$ clusters to form a 1S_0 state between them. In the ${}^3\text{He} + {}^2\text{H}$ system the role of the triplet forces is known to be very strong, causing the existence of the low-lying $3/2^+$ resonance [17]. The triplet forces, which have negligible effects in our present model, could

play a role if the small D -state admixture of ${}^3\text{He}$ were to be considered. In such a case one can have a contribution from coupling between the $\left\{ \left[(1, 1/2) 1/2, 0 \right] 1/2; \left[(1, 1/2) 3/2, 2 \right] 1/2 \right\}$ configurations in the ${}^3\text{He} + {}^3\text{He}$ system. Here the $\left[(S_d, S_p) S, l \right] I$ coupling scheme is used, with S_d and S_p being the deuteron and proton spins, respectively, S is the total intrinsic spin, l is the angular momentum between the deuteron and the proton, I is the total spin of ${}^3\text{He}$, and the brackets denote angular momentum coupling. Such a model would require a four-cluster description of ${}^3\text{He} + {}^3\text{He} = (d + p) + (d + p)$, which is beyond the scope of the present work. The effects of the internal D states in ${}^3\text{He}$ on the ${}^3\text{He} + {}^3\text{He}$ system will be studied in the future [18].

In many respects ${}^3\text{He} + {}^3\text{He}$ is similar to the $n + n$ system. We know that there is a virtual (antibound) state present in the $n + n$ system, with the wave number $k = -i\gamma$ ($\gamma > 0$) and energy $E = -E_V$ ($E_V > 0$) of the S -matrix pole, respectively. Such a state results in a cross section which is divergent at the unphysical negative pole energy and behaves as $\sigma \sim 1/(E + E_V)$ at positive energies. The effect of such a hypothetical state in ${}^3\text{He} + {}^3\text{He}$ on the ${}^3\text{He}({}^3\text{He}, 2p){}^4\text{He}$ cross section was discussed in Ref. [19]. It would lead to a cross section that increases with decreasing energy, mimicking the effect of electron screening. A closer look at the problem shows that pure virtual states (with pure imaginary wave number) cannot be present in Coulombic systems [20]. The Coulomb interaction creates two poles from the one virtual-state pole and moves them away from the imaginary k -axis to $k = \pm\kappa - i\gamma$ ($\gamma > 0$, $\kappa < \gamma$). Such states can still have observable effects, like in the $p + p$ system, because these conjugate poles are roughly at the same distance from the physical energies. We have searched for such states in ${}^3\text{He} + {}^3\text{He}$, and found no unambiguous evidence for their existence close to the imaginary k axis.

In summary, we do not find any S -matrix poles in either ${}^4\text{He} + p + p$ or ${}^3\text{He} + {}^3\text{He}$ that could cause strong observable effects in the ${}^3\text{He}({}^3\text{He}, 2p){}^4\text{He}$ cross section. For ${}^4\text{He} + p + p$ our result is probably the best, one can currently achieve. Further studies of ${}^3\text{He} + {}^3\text{He}$ in a $(d + p) + (d + p)$ model or in a full six-body dynamical model would be interesting.

IV. THE ${}^3\text{He}({}^3\text{He}, 2p){}^4\text{He}$ AND ${}^3\text{H}({}^3\text{H}, 2n){}^4\text{He}$ REACTION CROSS SECTIONS

${}^3\text{He}({}^3\text{He}, 2p){}^4\text{He}$ is the only solar nuclear reaction whose cross section has been measured within the solar Gamow window (around ≈ 20 keV). At such low energies the cross section, measured in the laboratory, is enhanced due to screening effects by the electrons present in the target atoms [21]. This electron screening effect has definitely been identified in the latest LUNA data for ${}^3\text{He}({}^3\text{He}, 2p){}^4\text{He}$. For applications in the solar models the electron screening enhancement has to be subtracted from the data.

Currently the ${}^3\text{He}(d, p){}^4\text{He}$ reaction is the one for which the enhancement of the low-energy fusion cross section due to electron screening is studied best. In agreement between experiment [22] and theory [23–25] it appears that the screening enhancement for this reaction, in which deuterons collide with an atomic ${}^3\text{He}$ gas target, is well described in the adiabatic limit. In this case the electron screening can be represented by a constant shift of the collision energy by the screening energy U_e which is given by the difference of the electronic binding energy of the united atom and the sum of the asymptotic fragments. Applied

to the ${}^3\text{He} + {}^3\text{He}$ reaction, the screening energy in the adiabatic limit is $U_e = 240$ eV. We will use this value in the following, but we note that fits to the LUNA data might indicate a somewhat larger screening potential [7,33]. These fits had to make assumptions about the energy dependence of the bare-nuclear ${}^3\text{He}({}^3\text{He}, 2p){}^4\text{He}$ S factor. This has motivated us to perform calculations for the bare reaction cross sections of ${}^3\text{He}({}^3\text{He}, 2p){}^4\text{He}$ and the mirror reaction ${}^3\text{H}({}^3\text{H}, 2n){}^4\text{He}$.

As we mentioned, a microscopic description of ${}^3\text{He}({}^3\text{He}, 2p){}^4\text{He}$, which handles the full three-body final state rigorously, is currently not feasible. Here we use a simplified version of the continuum-discretized coupled channel method [26] to describe ${}^4\text{He} + N + N$. In this method the total energy available for ${}^4\text{He} + N + N$ is divided between the ${}^4\text{He} - N$ and $({}^4\text{He}, N) - N$ relative motions in the $({}^4\text{He}, N)N$ configuration, and between the $N - N$ and $(N, N) - {}^4\text{He}$ motions in the $(N, N){}^4\text{He}$ configuration. Within the two-cluster subsystems, $({}^4\text{He}, N)$ or (N, N) , the continuum energy is discretized, and the remaining energy appears as the scattering energy in the $({}^4\text{He}, N) - N$ and $(N, N) - {}^4\text{He}$ two-body systems. The system of coupled channels is built up from the $({}^4\text{He}, N) - N$ and $(N, N) - {}^4\text{He}$ channels containing the various discretized-energy states in the two-cluster subsystems.

Generally, the discretization of the continuum in the two-body subsystems is done in equidistant k bins, and proper continuum states are used. Here we adopt a simpler approach. We discretize the continuum on a finite square-integrable basis. Thus, our discretized states are pseudo-bound states with square-integrable wave functions and positive energy. The discretization is performed by choosing N_d basis states with ranges that increase following a geometric progression. By varying the total range of the basis and N_d one can achieve very different discretization patterns, e.g., dense or sparse discretization, discretizations including only low energies or allowing high off-the-energy-shell states also, etc. This way one can test the sensitivity of the calculated reaction cross section on the continuum discretization, and see if this approximation is reasonable or not. We typically use $N_d = 5 - 10$ and solve the coupled-channel scattering problem by using the method of Ref. [16].

Figure 2 shows our results for ${}^3\text{He}({}^3\text{He}, 2p){}^4\text{He}$ and ${}^3\text{H}({}^3\text{H}, 2n){}^4\text{He}$ together with the available experimental data. In order to get rid of the the trivial exponential dropping of the cross sections caused by the Coulomb penetration, we use the astrophysical S -factor parametrization

$$S(E) = \sigma(E)E \exp[2\pi\eta(E)], \quad \eta(E) = \frac{\mu Z_1 Z_2 e^2}{k\hbar^2}. \quad (4)$$

Our curves in Fig. 2 come from a continuum discretization that proved to be the most stable at the $({}^4\text{He}, N) - N$ and $(N, N) - {}^4\text{He}$ two-body scattering level. We also tried other discretization patterns and found that the absolute normalization of the cross section curves depend somewhat (10–20%) on the chosen discretization, but the shapes of the curves remain very similar. Our results are close to those of Ref. [9], where a similar model was used. Our full model space is roughly 5–10 times bigger than in Ref. [9], which allows us to use much more flexible continuum discretizations. Nevertheless, all our results seem to be similar to Ref. [9], e.g., we also find that the channels involving the ${}^4\text{He} + N$ states with $J^\pi = 1/2^-$ have a dominant role.

Fig. 3 shows the effect of electron screening on our calculated ${}^3\text{He}({}^3\text{He}, 2p){}^4\text{He}$ S factor with $U_e = 240$ eV screening potential. A nice agreement is observed with the low-energy

LUNA data.

The overall agreement between our results and the experimental data is considered to be good. We see, however, a marked disagreement with the ${}^3\text{H}({}^3\text{H}, 2n){}^4\text{He}$ data at very low energies. The energy dependence of our calculated S factor is different from the precise Los Alamos data. One possible explanation of this discrepancy could be our approximate treatment of the three-body final state. However, this is not supported by our finding that the shape of the $S(E)$ curve is rather insensitive to the way the discretization is done. Nevertheless, an improved model with the full three-body treatment of the final state would be desirable. As we mentioned, the thresholds of the ${}^4\text{He}+n+n$ and ${}^3\text{H}+{}^3\text{H}$ channels are too far from each other in our model. In order to see if this may affect the energy-dependence of the S factor, we made some test calculations. We artificially modified the energies of the ${}^3\text{H}$ clusters to reproduce the experimental threshold energy difference. This changed the absolute normalization of the S factor (as the $3/2^-$ and especially the $1/2^-$ discretized states moved closer to the ${}^3\text{H}+{}^3\text{H}$ threshold) but not its shape.

V. CONCLUSION

We have studied the ${}^3\text{He}({}^3\text{He}, 2p){}^4\text{He}$ and ${}^3\text{H}({}^3\text{H}, 2n){}^4\text{He}$ reactions within the microscopic cluster model using significantly larger model spaces than previously employed. Our motivation and results have been twofold:

We searched for signs of possible low-energy resonances in ${}^3\text{He}({}^3\text{He}, 2p){}^4\text{He}$, which could have important effects on the ${}^7\text{Be}$ and ${}^8\text{B}$ solar neutrino fluxes. The ${}^3\text{He}+{}^3\text{He}$ and ${}^4\text{He}+p+p$ channels were studied separately, which allowed us to use methods that can treat the two- and three-body asymptotics in a rigorous way. We extended the two- and three-body scattering matrices to complex energies and searched for their poles. We have not found any indication for the existence of a low-energy resonance or virtual state that could cause observable effects in the cross section. Thus, it is unlikely that a yet unobserved resonance around the threshold energy in the ${}^3\text{He}({}^3\text{He}, 2p){}^4\text{He}$ reaction might affect this important solar reaction cross section.

We calculated the cross sections of the ${}^3\text{He}({}^3\text{He}, 2p){}^4\text{He}$ and ${}^3\text{H}({}^3\text{H}, 2n){}^4\text{He}$ reactions in the continuum-discretized coupled channel approximation. Our results are in a good general agreement with available data, except for the very low-energy ${}^3\text{H}({}^3\text{H}, 2n){}^4\text{He}$ cross section, where we observe a systematic deviation from the most precise measurement. Our test calculations show that the energy dependence of the cross sections is hardly influenced by the details of the continuum discretization, but might be caused by the approximate treatment of the 3-body continuum. Here improvements are certainly warranted.

ACKNOWLEDGMENTS

The work of A. C. was performed under the auspices of the U.S. Department of Energy and was supported by OTKA Grant F019701 and by the Bolyai Fellowship of the Hungarian Academy of Sciences. We also thank the Danish Research Council and the Theoretical Astrophysics Center for financial support.

REFERENCES

- [1] R. Davis Jr., Nucl. Phys. B (Proc. Suppl.) 48 (1996) 284; Y. Suzuki, Nucl. Phys. B (Proc. Suppl.) 38 (1995) 54; P. Anselmann et al., Phys. Lett. B 342 (1995) 440; J. N. Abdurashitov et al., Phys. Lett. B 328 (1994) 234.
- [2] J. N. Bahcall and M. H. Pinsonneault, Rev. Mod. Phys. 67 (1995) 781; S. Turck-Chièze, W. Däppen, E. Fossat, J. Provost, E. Schatzman and D. Vignaud, Phys. Rep. 230 (1993) 57; V. Castellani, S. Degl’Innocenti, G. Fiorentini, M. Lissia and B. Ricci, Phys. Rep. 281 (1997) 310.
- [3] N. Hata and P. Langacker, Phys. Rev. D 56 (1997) 6107.
- [4] J. N. Bahcall, Neutrino astrophysics (Cambridge University Press, Cambridge, 1989).
- [5] R. S. Raghavan, Science 267 (1995) 45.
- [6] W. A. Fowler, Nature 238 (1972) 24; V. N. Fetisov and Y. S. Kopysov, Phys. Lett. B 40 (1972) 602.
- [7] M. Junker, Phys. Rev. C 57 (1998) 2700; C. Arpesella et al., Phys. Lett B 389 (1996) 452.
- [8] S. Typel, G. Blüge, K. Langanke and W. A. Fowler, Z. Phys. A 339 (1991) 249.
- [9] P. Descouvemont, Phys. Rev. C 50 (1994) 2635.
- [10] D. R. Thompson, M. LeMere and Y. C. Tang, Nucl. Phys. A 268 (1977) 53; I. Reichstein and Y. C. Tang, Nucl. Phys. A 158 (1970) 529.
- [11] A. Csótó, Phys. Rev. C 49 (1994) 3035.
- [12] J. Aguilar and J. M. Combes, Commun. Math. Phys. 22 (1971) 269; E. Balslev and J. M. Combes, Commun. Math. Phys. 22 (1971) 280; B. Simon, Commun. Math. Phys. 27 (1972) 1.
- [13] S. Aoyama, S. Mukai, K. Katō, and K. Ikeda, Prog. Theor. Phys., 93 (1995) 99; 94 (1995) 343; K. Katō, S. Aoyama, S. Mukai, and K. Ikeda, Nucl. Phys. A 588 (1995) c29; B. V. Danilin, T. Rogde, S. N. Ershov, H. Heiberg-Andersen, J. S. Vaagen, I. J. Thompson, and M. V. Zhukov, Phys. Rev. C 55 (1997) R577; S. N. Ershov, T. Rogde, B. V. Danilin, J. S. Vaagen, I. J. Thompson, and F. A. Gareev, Phys. Rev. C 56 (1997) 1483; B. V. Danilin, I. J. Thompson, J. S. Vaagen, and M. V. Zhukov, Nucl. Phys. A 632 (1998) 383.
- [14] J. Jänecke et al., Phys. Rev. C 54 (1996) 1070.
- [15] A. Csótó, R. G. Lovas and A. T. Kruppa, Phys. Rev. Lett. 70 (1993) 1389; A. Csótó and G. M. Hale, Phys. Rev. C 55 (1997) 536.
- [16] M. Kamimura, Prog. Theor. Phys. Suppl. 62 (1977) 236.
- [17] G. Blüge and K. Langanke, Phys. Rev. C 41 (1990) 1191.
- [18] K. Varga and A. Csótó, to be published.
- [19] A. Csótó, e-print nucl-th/9712033.
- [20] G. M. Hale and A. Csótó, Phys. Rev. C, in press.
- [21] H. J. Assenbaum, K. Langanke, and C. Rolfs, Z. Phys. A 327 (1987) 461.
- [22] P. Prati et al., Z. Phys. A 350 (1994) 171.
- [23] T. D. Shoppa, S. E. Koonin, K. Langanke and R. Seki, Phys. Rev. C 48 (1993) 837.
- [24] K. Langanke, T. D. Shoppa, C. A. Barnes and C. Rolfs, Phys. Lett. B 369 (1996) 211.
- [25] J. Bang, L. S. Ferreira, E. Maglione and J. M. Hansteen, Phys. Rev. C 53 (1996) R18.

- [26] N. Austern, Y. Iseri, M. Kamimura, M. Kawai, G. Rawitscher and M. Yahiro, Phys. Rep. 154 (1987) 125.
- [27] A. Krauss, H. W. Becker, H. P. Trautvetter and C. Rolfs, Nucl. Phys. A 467 (1987) 273.
- [28] M. R. Dwarakanath, Phys. Rev. C 9 (1974) 805.
- [29] R. E. Brown and N. Jarmie, Radiat. Eff. 92 (1986) 45; N. Jarmie and R. E. Brown, Nucl. Inst. Meth. B 10-11 (1985) 405.
- [30] H. M. Agnew et al., Phys. Rev. 84 (1951) 862.
- [31] V. I. Serov, S. N. Abramovich and L. A. Morkin, Sov. J. At. Energy 42 (1977) 66.
- [32] A. M. Govorov, K. Li, G. M. Ostetinskii, V. I. Salatski and I. V. Sozor, Sov. Phys. JETP 15 (1962) 266.
- [33] C. Angulo and P. Descouvemont, Nucl. Phys. A 639 (1998) 733.

FIGURES

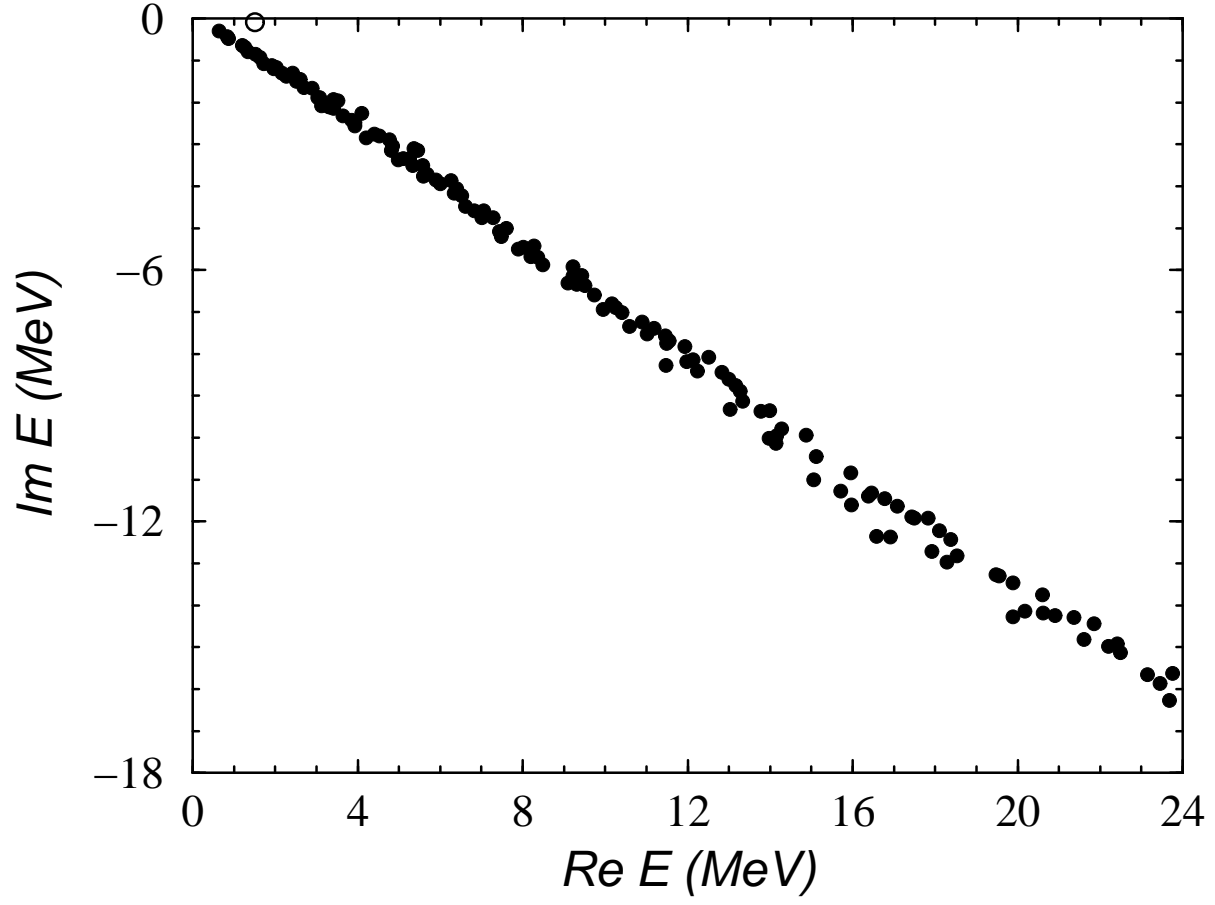


FIG. 1. Energy-eigenvalues of the complex scaled Hamiltonian of the $J^\pi = 0^+$ states in ${}^4\text{He} + p + p$. The dots are the points of the rotated discretized continuum, while the circle is the ground state resonance of ${}^6\text{Be}$.

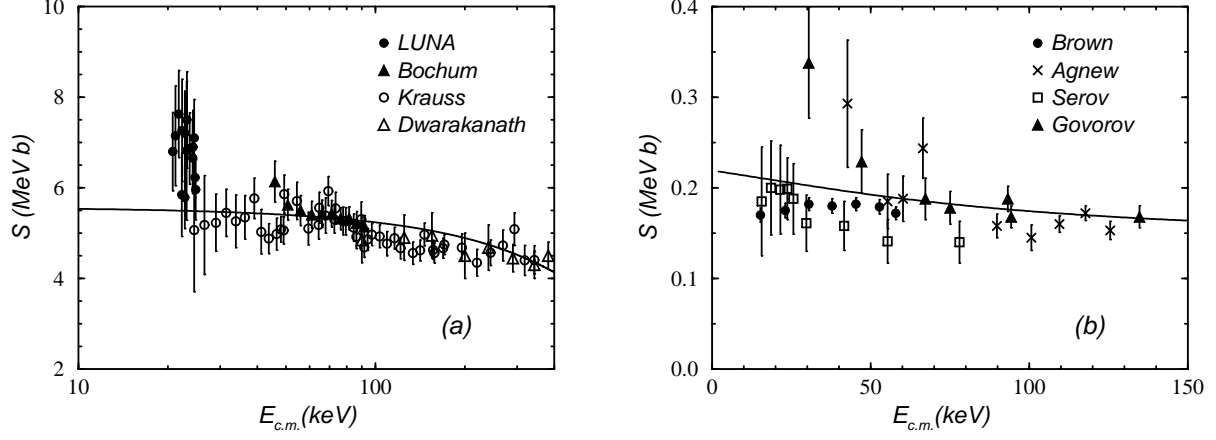


FIG. 2. Astrophysical S factors for the (a) ${}^3\text{He}({}^3\text{He}, 2p){}^4\text{He}$ and (b) ${}^3\text{H}({}^3\text{H}, 2n){}^4\text{He}$ reactions. The experimental data are taken from (a) [7] (filled circle, and filled triangle), [27] (open circle), [28] (open triangle) and (b) [29] (filled circle), [30] (cross), [31] (square), and [32] (triangle). The solid curves are our results.

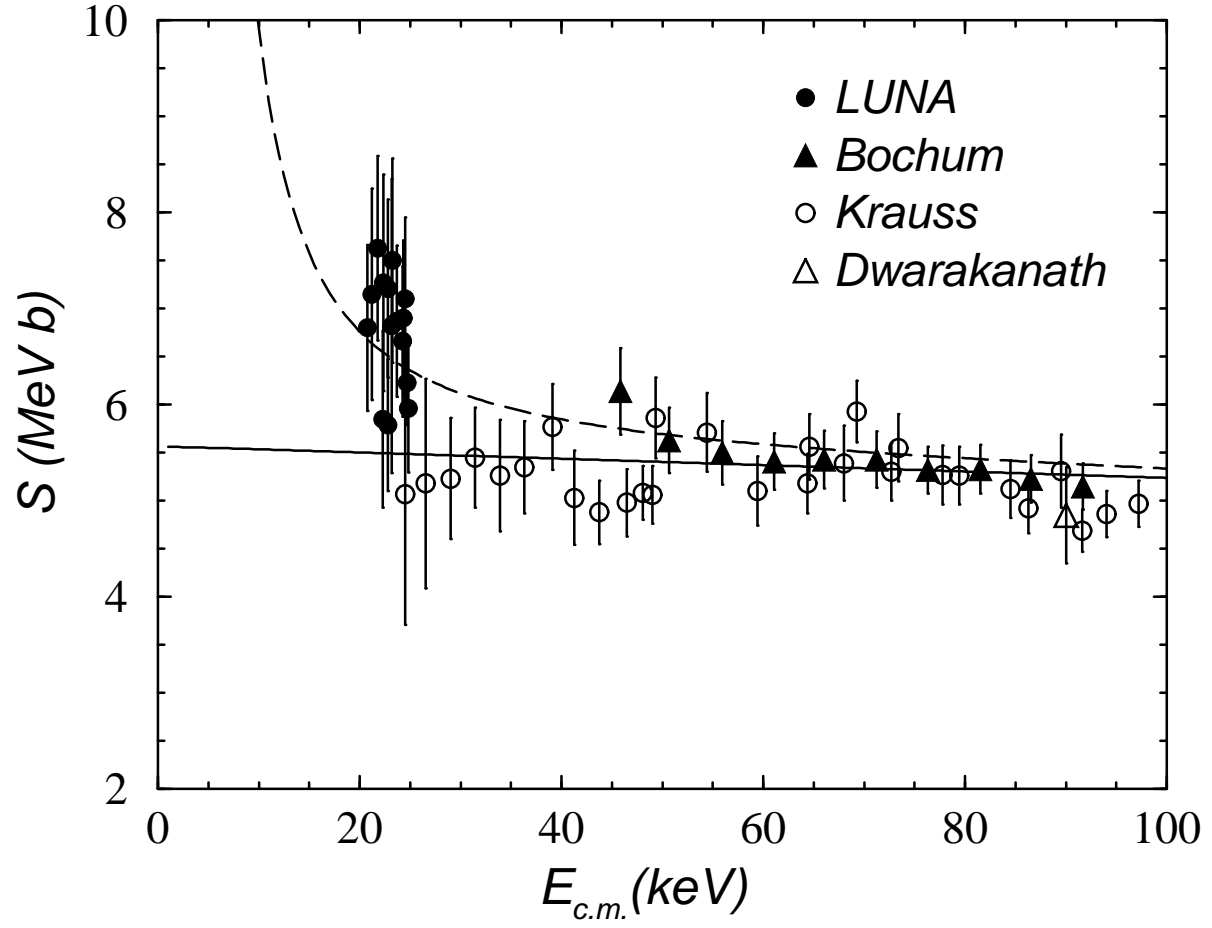


FIG. 3. The same as Fig. 2(a), except that the effect of electron screening on our low-energy theoretical curve is shown by the dashed line. The adiabatic screening potential, $U_e = 240 \text{ eV}$, is used.